ELSEVIER

Composite Structures 41 (1998) 273–284

COMPOSITE STRUCTURES

Investigation of composite box beam dynamics using a higher-order theory

Thomas R. McCarthy, Aditi Chattopadhyay

Department of Mechanical and Aerospace Engineering, Arizona State University, Tempe, AZ 85287-6106, USA

Abstract

A higher-order composite box beam theory is developed to model beams with arbitrary wall thicknesses. The theory, which is based on a refined displacement field, approximates the three-dimensional elasticity solution so that the beam cross-sectional properties are not reduced to one-dimensional beam parameters. Both inplane and out-of-plane warping are included automatically in the formulation. The model can accurately capture the tranverse shear stresses through the thickness of each wall while satisfying stress-free boundary conditions on the inner and outer surfaces of the beam. Numerical results are presented for beams with varying wall thicknesses and aspect ratios. The static results are correlated with available experimental data and show excellent agreement. Dynamic results presented show the importance of including inplane and out-of-plane warping deformations in the formulation.

1. Nomenclature

A_{ij}	Zeroth order laminate stiffness matrix (lb/in.)
B_{ij}	First order laminate stiffness matrix (lb)
c	Beam width (in.)
d	Beam height (in.)
D_{ij}	Second order laminate stiffness matrix (lb-in.)
E_{ij}	Third order laminate stiffness matrix (lb-in.^{2})
e°	Zeroth order strain tensor
$\mathbf{f}$	Forcing vector (lb)
F_{ij}	Fourth order laminate stiffness matrix (lb-in.^{3})
h	Wall thickness (in.)
H_{ij}	Sixth order laminate stiffness matrix (lb-in.^{5})
$\mathbf{K}$	Stiffness matrix (lb-in.)
L	Beam length (in.)
$\mathbf{M}$	Mass matrix (slugs)
O_{ij}	Seventh order laminate stiffness matrix (lb-in.^{6})
P_{ij}	Eighth order laminate stiffness matrix (lb-in.^{7})
$\mathbf{q}$	Nodal degree of freedom vector
Q_{ij}	Constitutive matrix (psi)
$\mathbf{S}$	Nodal displacement relationship matrix
T	Kinetic energy (lb-in.)
$\mathbf{T}_{ur}$	Transformation matrix between the displacements
$\hat{\mathbf{T}}_{ij}$	Transformation matrix between the strains
$\hat{t}_1, \hat{t}_2, \hat{t}_3$	Applied surface tractions (lb/in.^{2})
U	Strain energy (lb-in.)
u_1, u_2, u_3	Local displacements (in.)
U_0	Strain energy density (psi)
u_0, v_0, w_0	Displacements at midplane of walls (in.)
W_e	Applied external work (lb-in.)
X, Y, Z	Global coordinate system
X', Y', Z'	Global, rotated coordinate system
$\mathbf{X}_1, \mathbf{X}_2, \mathbf{X}_3$	Body forces (lb/in.^{3})
x, y, z	Local, untwisted coordinate system
$\boldsymbol{\beta}$	Nodal strain relationship matrix
χ, η, ζ	Local, twisted coordinate system
ε	Strain tensor
$\tilde{\varepsilon}'_j$	Strain in the local, twisted coordinate
$\kappa^1, \kappa^2, \kappa^3$	Higher order strain tensors (1/in., 1/in.^{2} and 1/in.^{3})
$\tilde{u}_j$	Additional strain components due to pre-twist
σ	Stress tensor (psi)

0263-8223/98/$ — see front matter
PII: S0263-8223(98)00041-5

ψ_x, ψ_y Higher-order displacement functions (rad.)
θ Twist by an angle (rad.)

2. Introduction

Composite materials are becoming increasingly popular for use as structural members in aircraft applications. Owing to the high strength-to-weight ratio offered by composites, structural weight is much less of an issue than it is for isotropic materials. Therefore it is no longer necessary to use thin-walled sections to model the load-carrying sections. Thus, it is essential to develop a general framework for the comprehensive analysis of such composite structures of arbitrary wall thickness.

Beam theories associated with isotropic materials have been well understood for years and these theories tend to predict the structural and dynamic response quite accurately [1]. Recently research has also been reported in deriving composite beam theories [2–10]. Among these, the more comprehensive anisotropic theories rely on a full three-dimensional finite element solution which can become very computationally intensive [1,2]. Reference [4] addresses comprehensive modeling of beams with solid cross-sections using a full three-dimensional finite element solution technique. In Ref. [5], a comprehensive finite element method based on the variational–asymptotical approach is used to model beams of arbitrary cross-sections. The theory includes warping terms, in addition to the extension and rotations of the beam, in which the average contribution of the warping over the cross-section of the beam is assumed to be zero. In the variational asymptotical approach, the three-dimensional properties of the beam are reduced to one-dimensional beam properties (extension, twist and two bending terms) and the beam response is then approximated based on an one-dimensional analysis. Results presented for thin-walled composite beams using this technique show very good correlation.

In other analysis of closed sections [6–10], as well as in some of the three-dimensional finite element models [2], the classical laminate theory (CLT) is used to model the individual plate elements of each beam. This theory, which neglects transverse shear effects, is only appropriate for thin laminates. However, as shown by Gu and Chattopadhyay [11], in case of anisotropic material, the changes in interlamina stiffnesses lead to transverse shear stresses even for 'so-called' thin laminates.

The objective of this research is to develop a more general, but computationally efficient, theory for the adequate analysis of composite box beam sections with moderately thick walls. A refined higher order displacement field is used to accurately represent the transverse shear stress distribution in composite laminates of arbitrary thickness. Based on this, a procedure is developed for the analysis of moderately thick walled rectangular composite box beam sections with pre-twist, taper and sweep to model load carrying structural members used in aerospace applications. Unlike the beam theory described in Ref. [5], the proposed theory approximates the three-dimensional elasticity solution rather than reducing the beam properties to one-dimensional quantities. Further, the warping of the cross-section in this theory is determined such that stress free boundary conditions are exactly satisfied on the inner and the outer surfaces.

3. Problem Formulation

A single-celled composite box beam analysis is developed using a higher order composite laminate theory [12] which accounts for the distributions of shear strains through the thicknesses of each wall. Individual displacement fields are assumed for each of the four box beam walls (Fig. 1). Continuity between the displacement fields is enforced at each of the four corners throughout the thickness of each plate. By using the higher-order laminate theory in each wall, the solution of cross-sectional deformations are an approximation of the exact elasticity approach. In this regard, the standard beam degrees of freedom (extension, twist and two bending terms) are not used. However, the cross-section of the beam is described fully by stretching, bending, twisting, shearing and both inplane and out-of-plane warping. Since the analysis is capable of modeling composite box beams of moderately large thicknesses, the model accurately describes

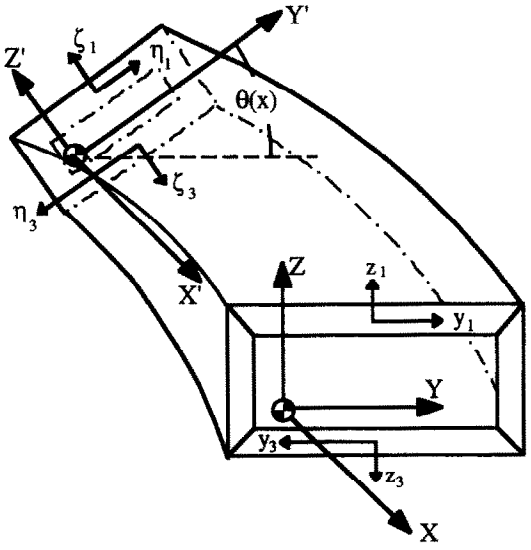

Fig. 1. Composite box beam.

moderately thick-walled load-carrying members currently being used in aerospace applications. The procedure is developed for short aspect ratio beams, therefore, using a two-dimensional finite element model, the beam is discretized with unequal element sizes to accurately describe arbitrary spanwise distributions.

4. Composite structural modeling

The box beam is modeled using composite laminates representing the four walls (Fig. 1). Several different coordinate systems are used throughout this paper and are defined as follows. The global coordinate system (X, Y, Z) is the untwisted coordinate system which is located on the axis of rotation (Figs. 1 and 2). The global, rotated coordinate system (X′, Y′, Z′) represents the coordinate system defined when the global coordinate system is rotated about the axis of twist by an angle $\theta(x)$. There are also two coordinate systems defined locally in each wall of the box beam. The local, untwisted coordinate system of the ith wall is defined by (x_i, y_i, z_i). The local, twisted wall coordinate system for the ith wall which results from the global rotation (θ) of the beam is denoted (χ_i, η_i, ζ_i) as depicted in Fig. 1 (shown for the horizontal walls only). Detailed explanations of the transformations between the coordinate systems are found in Appendix A.

4.1. *Higher-order theory*

The displacement field for each wall is defined in the local, twisted coordinate system (χ, η, ζ) as follows, where the subscript 'i' has been omitted for convenience throughout the remainder of the paper.

$$\tilde{u}_1(\chi,\eta,\zeta) = u_0(\chi,\eta) + \zeta\left(-\frac{\partial u_3(x,\eta)}{\partial \chi} + \psi_x(\chi,\eta)\right) + \zeta^2\phi_x(\chi,\eta) + \zeta^3\gamma_x(\chi,\eta) \tag{1a}$$

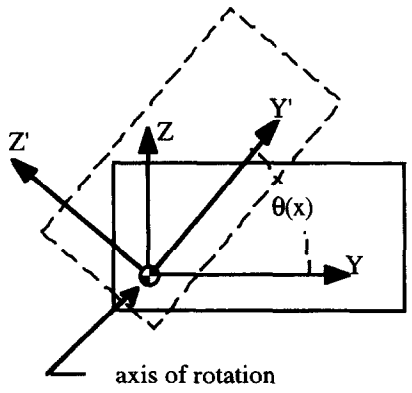

Fig. 2. Beam cross-section and axis of rotation.

$$\tilde{u}_2(\chi,\eta,\zeta) = v_0(\chi,\eta) + \zeta\left(-\frac{\partial u_3(x,\eta)}{\partial \eta} + \psi_y(\chi,\eta)\right) + \zeta^2\phi_y(\chi,\eta) + \zeta^3\gamma_y(\chi,\eta) \tag{1b}$$

$$\tilde{u}_3(\chi,\eta) = w_0(\chi,\eta) \tag{1c}$$

where u_0, v_0 and w_0 represent the displacements at the midplane of each plate and ψ_x and ψ_y represent the rotations of the normals to the midplane. The beam warping in each plate is represented by the functions ϕ_x, ϕ_y, γ_x and γ_y. The local wall deformations ($\tilde{u}_1$, $\tilde{u}_2$, $\tilde{u}_3$) in the twisted coordinate system are related to local deformations (u_1, u_2, u_3) in the untwisted coordinate system (x, y, z) through the following relationship.

$$\begin{Bmatrix} u_1 \\ u_2 \\ u_3 \end{Bmatrix} = \begin{bmatrix} 1 & 0 & 0 \\ 0 & \cos\theta & -\sin\theta \\ 0 & \sin\theta & \cos\theta \end{bmatrix} \begin{Bmatrix} \tilde{u}_1 \\ \tilde{u}_2 \\ \tilde{u}_3 \end{Bmatrix} \tag{2}$$

or

$$\mathbf{u} = \mathbf{T}_{ur}\tilde{\mathbf{u}}$$

where $\mathbf{T}_{ur}$ is the transformation matrix from the local, twisted displacements to the local, untwisted displacements.

4.2. *Boundary conditions*

The higher-order functions (ϕ_x, ϕ_y, γ_x and γ_y) are determined based on the condition that the transverse shear stresses, $\sigma_{\chi\zeta}$ and $\sigma_{\eta\zeta}$, vanish on the inner and outer surfaces of the beam. For composite laminates made up of layers of orthotropic lamina, this is equivalent to the requirement that the corresponding strains be zero on these surfaces. Using the stress-free boundary conditions, it can be shown that the original displacement field (eqns (1a)–(1c)) is reduced to the following set of equations.

$$\tilde{u}_1 = u_0 + \zeta\left(-\frac{\partial w_0}{\partial \chi} + \psi_x\right) - \frac{4}{3h^2}\zeta^3\psi_x \tag{3a}$$

$$\tilde{u}_2 = v_0 + \zeta\left(-\frac{\partial w_0}{\partial \chi} + \psi_y\right) - \frac{4}{3h^2}\zeta^3\psi_y \tag{3b}$$

$$\tilde{u}_3 = w_0 \tag{3c}$$

where the functions u_0, v_0, w_0, ψ_x and ψ_y represent unknown functions of χ and η.

4.3. *Stress-strain relations*

Owing to the fact that the stress and strain tensors are symmetric there are only six unique values of these quantities. Therefore, the following notation is used to

define the stress and strain tensors in the local, untwisted coordinate system.

$$\begin{Bmatrix}\sigma_1\\ \sigma_2\\ \sigma_3\\ \sigma_4\\ \sigma_5\\ \sigma_6\end{Bmatrix}^T = \begin{Bmatrix}\sigma_{xx}\\ \sigma_{yy}\\ \sigma_{zz}\\ \sigma_{yz}\\ \sigma_{xz}\\ \sigma_{xy}\end{Bmatrix}^T \quad \text{and} \quad \begin{Bmatrix}\varepsilon_1\\ \varepsilon_2\\ \varepsilon_3\\ \varepsilon_4\\ \varepsilon_5\\ \varepsilon_6\end{Bmatrix}^T = \begin{Bmatrix}\varepsilon_{xx}\\ \varepsilon_{yy}\\ \varepsilon_{zz}\\ 2\varepsilon_{yz}\\ 2\varepsilon_{xz}\\ 2\varepsilon_{xy}\end{Bmatrix}^T \tag{4a,b}$$

The stress and strain tensors in the local, twisted coordinate system are expressed similarly. The generalized Hooke's law is used to relate the stress and the strain. Assuming the products of the derivatives of the displacements to be small in the strain formulation, the following relationship is obtained between the local strains in the untwisted and the twisted coordinate systems.

$$\tilde{\varepsilon}_i = \tilde{T}_{ij}(\tilde{\varepsilon}_j^0 + \theta_{,x}\tilde{\mu}_j) \tag{5}$$

where $\tilde{\varepsilon}_j^0$ is the strain in the local, twisted coordinate in the absence of pre-twist, $\tilde{\mu}_j$ is the additional strain components due to pre-twist and $\theta_{,x}$ is the first derivative of the twist with respect to x. The total strain in the local, untwisted coordinate system (x, y, z) is denoted ε_j and $\tilde{T}_{ij}$ is the transformation matrix between the strains in the local, twisted coordinate system and the strains in the local, untwisted coordinate system. Note that the transformation matrix for the strains is not the same as the transformation matrix for the displacements (T_{ur}). The local inplane strains in the absence of pre-twist are derived as follows.

$$\begin{aligned}\tilde{\varepsilon}_1^0 &= e_1^0 + \zeta\kappa_1^1 + \zeta^3\kappa_1^3\\ \tilde{\varepsilon}_2^0 &= e_2^0 + \zeta\kappa_2^1 + \zeta^3\kappa_2^3\\ \tilde{\varepsilon}_6^0 &= e_6^0 + \zeta\kappa_6^1 + \zeta^3\kappa_6^3\end{aligned} \tag{6a–c}$$

The out of plane strains are expressed similarly.

$$\tilde{\varepsilon}_3^0 = 0 \tag{6d}$$

$$\tilde{\varepsilon}_4^0 = e_4^0 + \zeta^2\kappa_4^2 \tag{6e}$$

$$\tilde{\varepsilon}_5^0 = e_5^0 + \zeta^2\kappa_5^2 \tag{6f}$$

The additional strain due to beam pre-twist are as follows.

$$\tilde{\mu}_1 = \mu_1^0 + \zeta\mu_1^1 + \zeta^2\mu_1^2 + \zeta^3\mu_1^3 + \zeta^4\mu_1^4 \tag{7a}$$

$$\tilde{\mu}_2 = \tilde{\mu}_3 = \tilde{\mu}_4 = 0 \tag{7b–d}$$

$$\tilde{\mu}_5 = \mu_5^0 + \zeta\mu_5^1 + \zeta^3\mu_5^3 \tag{7e}$$

$$\tilde{\mu}_6 = \mu_6^0 + \zeta\mu_6^1 + \zeta^2\mu_6^2 + \zeta^3\mu_6^3 + \zeta^4\mu_6^4 \tag{7f}$$

where the individual strain components are described in Appendix B.

4.4. *Energy formulation*

The beam equations of motion are derived using Hamilton's principle [13] which assumes the following form.

$$\delta\int_{t_1}^{t_2}(U - T + W_e)\mathrm{d}t = 0 \tag{8}$$

where $\delta()$ represents the variation of () and U, T and W_e represent the total beam strain energy, kinetic energy and external work, respectively. Using variational principles, eqn (8) may be rewritten in terms of the individual plate quantities as follows.

$$\int_{t_1}^{t_2}\left(\sum_{i=1}^{N}\delta U_i - \delta T_i + \delta W_{e_i}\right)\mathrm{d}t = 0 \tag{9}$$

where N is the total number of walls ($N = 4$ for a box beam). The individual strain energy density (U_o) in each plate is calculated as follows.

$$U_0 = \int_0^{\varepsilon_i}\sigma_i\,\mathrm{d}\varepsilon_i = \int_0^{\varepsilon_i}Q_{ij}\varepsilon_j\,\mathrm{d}\varepsilon_i = \frac{1}{2}Q_{ij}\varepsilon_i\varepsilon_j \tag{10}$$

where repeated indices (i, $j = 1, 2, \ldots, 6$) indicate summation, σ_i is the strain tensor and Q_{ij} are the full three-dimensional material properties in the local, untwisted coordinate system. The material properties in terms of the local, untwisted coordinate system (x, y, z) may be written in terms of the material properties in local, twisted coordinate system (χ, η, ζ) as follows

$$Q_{ij} = T_{mi}\tilde{Q}_{mn}T_{nj} \tag{11}$$

where $\tilde{Q}_{mn}$ represents the material properties in the local, twisted coordinate system. The total strain energy of the ith wall (U_i) is then written, using eqn (5) and eqn (11) as

$$U_i = \int_V U_{o_i}\mathrm{d}V = \frac{1}{2}\int_V(\tilde{\varepsilon}_m^0 + \theta_{,x}\tilde{\mu}_m)T_{ik}T_{mi}\tilde{Q}_{mn}T_{nj}T_{jl} \times(\tilde{\varepsilon}_n^0 + \theta_{,x}\tilde{\mu}_n)\mathrm{d}V \tag{12}$$

where V indicates integration over the volume of the wall. Owing to the orthogonality of the transformation matrix, **T**, ($T_{ik}T_{mi} = \partial_{mk}$, where ∂_{mk} is the Kronecker delta) this equation is simplified as follows.

$$U_i = \frac{1}{2}\int_\Omega\int_{-h/2}^{h/2}(\tilde{\varepsilon}_m^0 + \theta_{,x}\tilde{\mu}_m)\tilde{Q}_{mn}(\tilde{\varepsilon}_n^0 + \theta_{,x}\tilde{\mu}_n)\mathrm{d}\zeta\mathrm{d}\Omega \tag{13}$$

where $d\Omega$ is the differential area ($d\Omega = d\chi d\eta$). The strain energy can be rewritten using eqns (6), (7) and (13).

$$U_i = \frac{1}{2}\int_\Omega \boldsymbol{\beta}_m^T \begin{bmatrix} A_{mn} & B_{mn} & D_{mn} & E_{mn} & F_{mn} \\ B_{mn} & D_{mn} & E_{mn} & F_{mn} & G_{mn} \\ D_{mn} & E_{mn} & F_{mn} & G_{mn} & H_{mn} \\ E_{mn} & F_{mn} & G_{mn} & H_{mn} & O_{mn} \\ F_{mn} & G_{mn} & H_{mn} & O_{mn} & P_{mn} \end{bmatrix} \boldsymbol{\beta}_n d\Omega \quad (14)$$

$$= \frac{1}{2}\int_\Omega \boldsymbol{\beta}_m^T Q_{mn} \boldsymbol{\beta}_n d\Omega$$

where m, $n = 1, 2, \ldots, 6$ and the laminate stiffness matrices (**A–P**) are defined in each of the walls as follows.

$$(\mathbf{A,B,D,E,F,G,H,O,P}) = \int_{-h/2}^{h/2} \tilde{\mathbf{Q}}(1,\zeta,\zeta^2,\zeta^3,\zeta^4,\zeta^5,\zeta^6,\zeta^7,\zeta^8)d\zeta \quad (15)$$

and the vector $\boldsymbol{\beta}_m$ is defined as

$$\boldsymbol{\beta}_m = [(e_m^0 + \mu_m^0\theta_{,x})(\kappa_m^1 + \mu_m^1\theta_{,x})(\kappa_m^2 + \mu_m^2\theta_{,x})(\kappa_m^3 + \mu_m^3\theta_{,x})\,\mu_m^4\theta_{,x}]^T \quad (16)$$

The external work due to applied loads and body forces (W_e) in the ith wall is written as

$$W_{e_i} = \int_V \bar{X}_j u_j dV + \int_{\mathscr{S}} \hat{t}_j u_j d\mathscr{S} \quad j = 1,2,3 \quad (17)$$

where u_j is the displacement vector defined as $[\tilde{u}_1, \tilde{u}_2, \tilde{u}_3]^T$, $\bar{X}_1$, $\bar{X}_2$ and $\bar{X}_3$ are the body forces in the X, Y and Z directions, respectively, and V represents the volume of the wall. Applied surface tractions over the region of the surface $\mathscr{S}$ are denoted $\hat{t}_1$, $\hat{t}_2$ and $\hat{t}_3$, along the respective directions.

The total kinetic energy of the beam is expressed as

$$T = \frac{1}{2}\int_V \rho v_i v_i dV \quad i = 1,2,3 \quad (18)$$

where $\boldsymbol{v}$ is the velocity vector defined as

$$\boldsymbol{v} = [\dot{\tilde{u}}_1, \dot{\tilde{u}}_2, \dot{\tilde{u}}_3]^T$$

and the notation $\dot{()}$ denotes a derivative with respect to time.

4.5. *Variational method*

The variation of strain energy is written as follows.

$$\delta U_i = \int_\Omega \boldsymbol{\beta}_m^T Q_{mn} \delta\boldsymbol{\beta}_n d\Omega \quad m,n = 1, 2, \ldots 6 \quad (20)$$

The variation of the strain vector $\boldsymbol{\beta}_m$ is expressed as the sum of the variation of the strain in the non-rotated coordinate system and the variation of the strain due to rotation as follows

$$\delta\boldsymbol{\beta}_m = [(\delta e_m^0 + \delta\mu_m^0\theta_{,x})(\delta\kappa_m^1 + \delta\mu_m^1\theta_{,x})(\delta\kappa_m^2 + \delta\mu_m^2\theta_{,x}) \times (\delta\kappa_m^3 + \delta\mu_m^3\theta_{,x})\,\delta\mu_m^4\theta_{,x}]^T \quad (21)$$

The variation of the potential energy of the applied loads is

$$\delta W_e = \int_V \bar{X}_i \delta u_i dV + \int_{\mathscr{S}} \hat{t}_i \delta u_i d\mathscr{S}. \quad i = 1,2,3 \quad (22)$$

Finally, the variation of the kinetic energy is written as

$$\delta T = \int_V \rho v_i \delta v_i dV \quad i = 1,2,3 \quad (23)$$

5. Solution procedure

The solution of equations of motion is obtained using a two-dimensional finite element formulation in the local, twisted coordinate system of each individual plate (χ, η, ζ). A four noded plate element is used to discretize the individual plates of the beam. This element is C^1 continuous in the zeroth order displacements (u_o, v_o, w_0) and is C^0 continuous for the higher order terms (ψ_x, ψ_y). As a result, the element contains 11 degrees of freedom per node which are defined in terms of the nodal degree of freedom vector as follows.

$$\mathbf{q} = \left[u_0, \frac{\partial u_0}{\partial\chi}, \frac{\partial u_0}{\partial\eta}, v_0, \frac{\partial v_0}{\partial\chi}, \frac{\partial v_0}{\partial\eta}, w_0, \frac{\partial w_0}{\partial\chi}, \frac{\partial w_0}{\partial\eta}, \psi_x, \psi_y\right]^T \quad (24)$$

5.1. *Continuity conditions*

To maintain the continuity of displacements throughout the entire beam, constraints are imposed at the corners of each individual plate as follows.

$$\begin{aligned} {}^1u_0(\chi,\eta = b_1) &= {}^2u_0(\chi,\eta = 0) \\ {}^1v_0(\chi,\eta = b_1) &= {}^2 - w_0(\chi,\eta = 0) \\ {}^1w_0(\chi,\eta = b_1) &= {}^2v_0(\chi,\eta = 0) \end{aligned} \quad (25a\text{–}c)$$

where the preceding superscripts 1 and 2 denote walls 1 and 2, respectively and b_1 is the width of wall 1. It must be noted that these equalities hold true for all χ and therefore the partial derivatives of the above equalities, with respect to χ, also represent constraints. To ensure that the angle between the walls remains 90°

after deformation, the following constraints are imposed on the rotations about the χ-axis.

$$^1w_{o,\eta}(\chi,\eta=b_1) = {}^2w_{o,\eta}(\chi,\eta=0)$$
$$^1\psi_y(\chi,\eta=b_1) = {}^2\psi_y(\chi,\eta=0)$$

Similar sets of constraints are derived at each of the four corners.

5.2. *Finite element formulation*

The finite element approach is used to solve the complete beam equations of motion (eqn (9)). Denoting $\boldsymbol{q}$ as the nodal degree of freedom vector, it is possible to express the strain (eqn (5)) in the following form

$$\tilde{\varepsilon}_i = (\Gamma_{ij} + \theta_{,x}\Phi_{ij})q_j \tag{27}$$

where Γ_{ij} are the nodal strain components and Φ_{ij} are the additional nodal srain components due to pre-twist. The partial derivatives of the strain with respect to q_j are then written as

$$\frac{\partial \tilde{\varepsilon} i}{\partial q_j} = \Gamma_{ij} + \theta_{,x}\Phi_{ij} \tag{28}$$

Note that quantities Γ and Φ can be expanded in terms of ζ as follows

$$\Gamma_{ij} = [\Gamma^o_{ij}\ \Gamma^1_{ij}\ \Gamma^2_{ij}\ \Gamma^3_{ij}\ \Gamma^4_{ij}]\bullet\{1\ \zeta\ \zeta^2\ \zeta^3\ \zeta^4\} = \mathscr{B}_{ij}\bullet\{1\ \zeta\ \zeta^2\ \zeta^3\zeta^4\} \tag{29}$$

and

$$\Phi_{ij} = [\Phi^0_{ij}\ \Phi^1_{ij}\ \Phi^2_{ij}\ \Phi^3_{ij}\ \Phi^4_{ij}]\bullet\{1\ \zeta\ \zeta^2\zeta^3\ \zeta^4\} = \mathscr{R}_{ij}\bullet\{1\ \zeta\ \zeta^2\ \zeta^3\ \zeta^4\} \tag{30}$$

Similarly, the displacement vector $\boldsymbol{u}$ may be written as

$$\tilde{u}_i = S_{ij}q_j \tag{31}$$

where S_{ij} are the components of the nodal displacement relationship matrix. The partial derivatives of the displacements with respect to q_j are as follows

$$\frac{\partial \tilde{u}_i}{\partial q_j} = S_{ij} \tag{32}$$

Using these relationships, the beam equations of motion are written in matrix form as

$$\mathbf{M}\ddot{\mathbf{q}} + \mathbf{K}\mathbf{q} = \mathbf{f} \tag{33}$$

where the mass and stiffness matrices are denoted

$$\mathbf{M} = \sum_{i=1}^{N}\left[\int_\Omega \rho \mathbf{S}^T\mathbf{S}d\Omega\right] \tag{34}$$

$$\boldsymbol{K} = \sum_{i=1}^{N}\left[\int_\Omega (\mathscr{B}^T + \theta_{,x}\mathscr{R}^T)Q(\mathscr{B} + \theta_{,x}\mathscr{R})d\Omega\right] \tag{35}$$

and the forcing vector is

$$\mathbf{f} = \sum_{i=1}^{N}\left[\int_\Omega \mathbf{T}_{ur}\mathbf{S}\mathbf{X}d\Omega + \int_{\mathscr{S}} \mathbf{T}_{ur}\mathbf{S}\hat{\mathbf{t}}d\mathscr{S}\right]. \tag{36}$$

6. Results

A static correlation with existing thin-walled composite box beam data is presented first in order to illustrate the accuracy of the model. Next, dynamic results are presented for a variety of both thin and thick-walled beams. Since an application of the developed theory includes modeling of the principal load-carrying member in rotor blade, the FPS units which are commonly used in rotary wing design are used in this paper.

6.1. *Static results*

To validate the developed procedure, a correlation study is made with available experimental results on a thin-walled box beam[14] and a previously developed analytical model[15]. The analytical model developed in Ref. [15] is a one-dimensional thin-walled beam model, based on the classical laminate theory (CLT), in which the out-of-plane warping effects are based on a contour analysis. The details of the beam studied are presented in Table 1. Figures 3 and 4 present the bending slope and induced twist, respectively, for a 1 lb vertical load at the tip. In Figs 5 and 6, the induced bending slope and elastic twist are presented for a 1 lb-in. tip moment. Very good agreement is observed between the results obtained using the present theory and the experimental data in most cases. It is also seen that results predicted in Ref. [15] are significantly lower than the experimental data, particularly for the induced twist due to the vertical tip load (Fig. 4). Further, the results are in excellent agreement with Cesnik et al. [5] whose variational asymptotical approach is well suited for this thin-walled box beam. This approach reduces the cross-sectional properties into one-dimensional beam properties based on an expansion in terms of a small parameter which is defined as the beam height divided by the beam length.

Table 1
Details of experimental beam[14]

Length = 30 in., width = 0.953 in., depth = 0.53 in.
ply thickness = 0.005 in., number of plies = 6
total wall thickness = 0.030 in, $E_1 = 20.59 \times 10^6$ psi,
$E_2 = 1.42 \times 10^6$ psi
$G_{12} = 0.89 \times 10^6$ psi, $G_{13} = 0.70 \times 10^6$ psi
$\eta_{12} = 0.42$, $\rho = 0.0502$ lb_m/in^3, Horizontal wall lay-up: $[45°]_6$
Vertical wall lay-up: $[45°/-45°]_3$

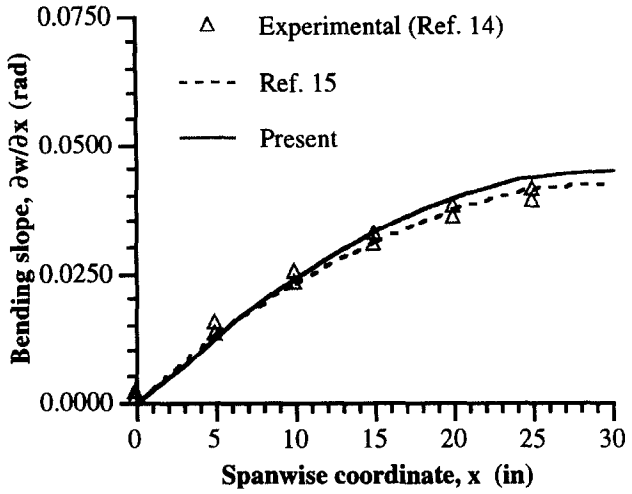

Fig. 3. Bending slope of $[45°]_6$ thin-walled beam under 1 lb bending load at tip.

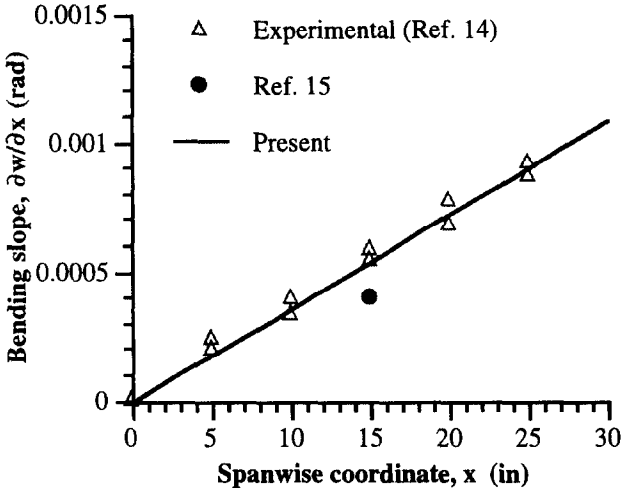

Fig. 5. Torsion-induced bending slope of $[45°]_6$ thin-walled beam under 1 in.-lb torsional moment at tip.

This theory includes both inplane and out-of-plane warping.

6.2. *Dynamic results*

To show the effect of inplane and out-of-plane warping on beam dynamic deformation, several interesting mode shapes are presented for the composite beam studied in Ref. [14]. To calculate the mode shapes, a finite element mesh of 10 × 4 elements is used in each plate. Owing to the stacking sequence of this composite beam (Table 1), flap-lag coupling is absent, however, both bending–torsion coupling and extension–shear coupling are present. Further, since the beam contains only ±45° plies, it is extremely rigid in torsion and the first torsional natural frequency (ω_{t1}) is 47.2 × the fundamental natural frequency (ω_o = 5.435 Hz). As a result, there is no warping, either inplane or out-of-plane, in the first five beam bending modes ($\omega_{b5} = 54.5\ \omega_1$) and in the first four chordwise bending modes ($\omega_{c5} = 57.5\ \omega_0$). To illustrate the lack of coupling and/or warping in the first several modes, the fourth chordwise bending mode is shown in Fig. 7. However, there exists a purely inplane warping mode which occurs before the second torsion mode ($\omega_{t2} = 122\ \omega_0$). This mode, whose natural frequency is 82.8 × the fundamental frequency, is illustrated in Fig. 8. The lack of significant out-of-plane warping for this composite beam is due to its thin-walled construction. Owing to the very thin walls, the beam bending motion is accounted for by pure bending in the horizontal walls and the chordwise bending motion is accounted for by pure bending in the vertical walls. The bending

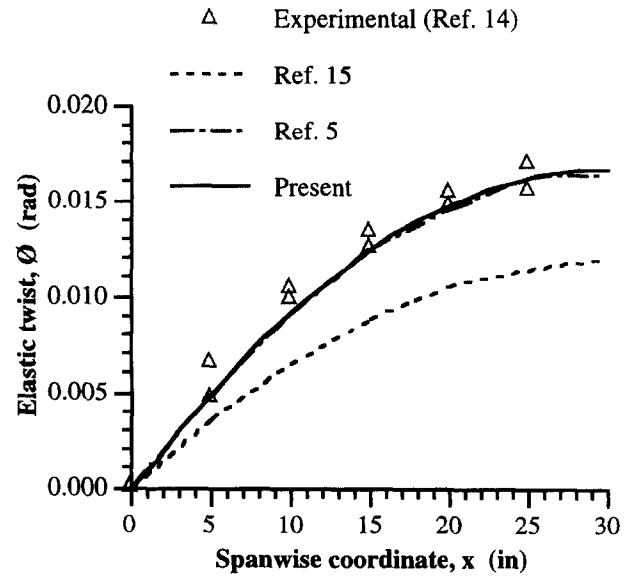

Fig. 4. Bending-induced twist of $[45°]_6$ thin-walled beam under 1 lb. bending load at tip.

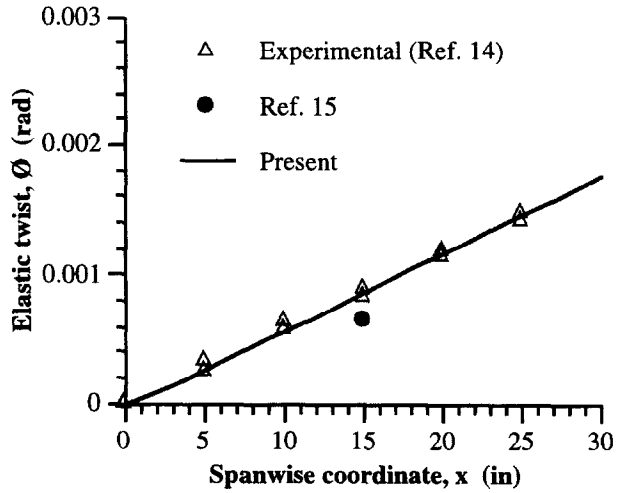

Fig. 6. Twist of $[45°]_6$ thin-walled beam under 1 in.-lb torsional moment at tip.

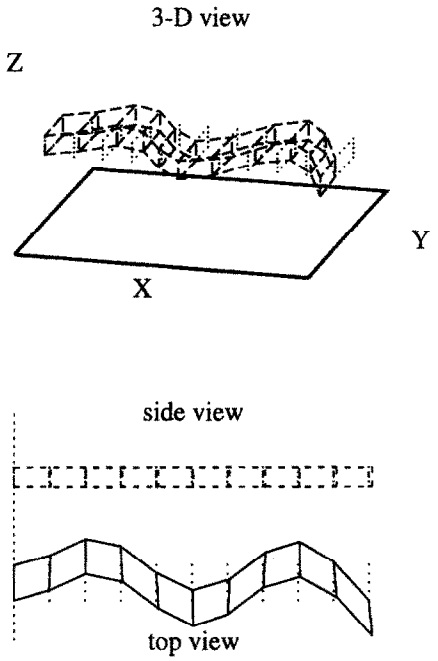

Fig. 7. Fourth chordwise bending mode of $[45°]_6$ thin-walled beam.

motions are much larger than any inplane shear in the walls and as a result there is very little warping.

In addition to the beams studied in Refs [14] and [15], mode shapes are also presented for a thicker and shorter version of the same beams with two different sets of material properties. Complete details of the beam dimensions are listed in Table 2. The first set of material properties corresponds to an isotropic beam. The isotropic material properties used for this study

Table 2
Details of moderately thick beam

Length = 10 in., width = 2 in., depth = 1 in.
ply thickness = 0.0667 in., number of plies = 6
total wall thickness = 0.4 in.
Isotropic material properties: $E = 10 \times 10^6$ psi, $\nu = 0.3$, $\rho = 0.1$ lb_m/in^3

are listed in Table 2. The second beam is made of orthotropic laminae with identical lay-up and material properties as those listed in Table 1.

In the isotropic beam case, it is seen from Fig. 9 that out-of-plane warping is present as early as in the second chordwise bending mode ($\omega_{c2} = 10.5\omega_0$, $\omega_0 = 91.8$ Hz). This out-of-plane warping is due to the presence of inplane shear in the side walls. The third torsional mode ($\omega_{t3} = 33.2\ \omega_0$) is presented in Fig. 10. A careful examination of this figure shows a small amount of both inplane and out-of-plane warping. This warping, which represents somewhat of a three-dimensional camber, is greatest near the node points. The camber effect is due to the shearing of the cross-section.

To investigate the effect of wall thickness on the warping of composite beams, mode shapes are calculated for a thicker and shorter composite beam with cross-sectional dimensions that are approximately twice that of the original beam studied in Ref. [14]. The length of the new beam is one-third that of the previous beam. The laminate stacking sequence and material properties are the same as those used in the

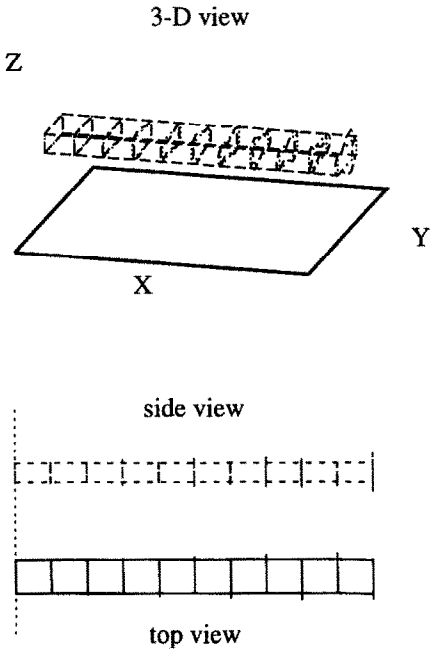

Fig. 8. Inplane warping mode of $[45°]_6$ thin-walled beam.

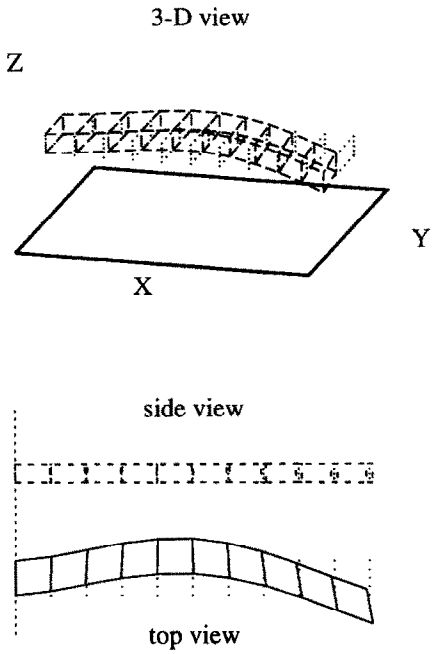

Fig. 9. Second chordwise bending mode of isotropic thick- walled beam.

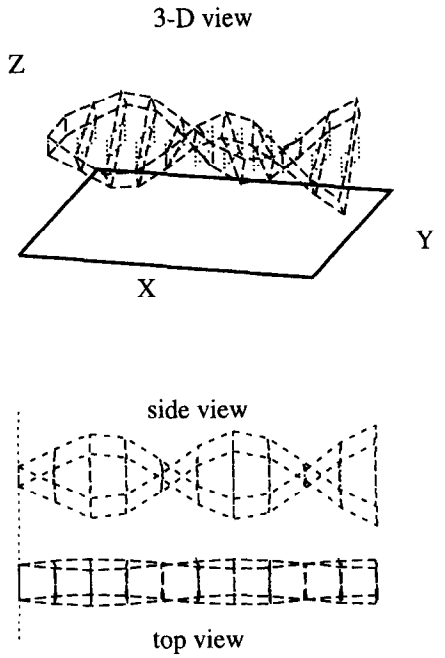

Fig. 10. Third torsion mode of isotropic thick-walled beam.

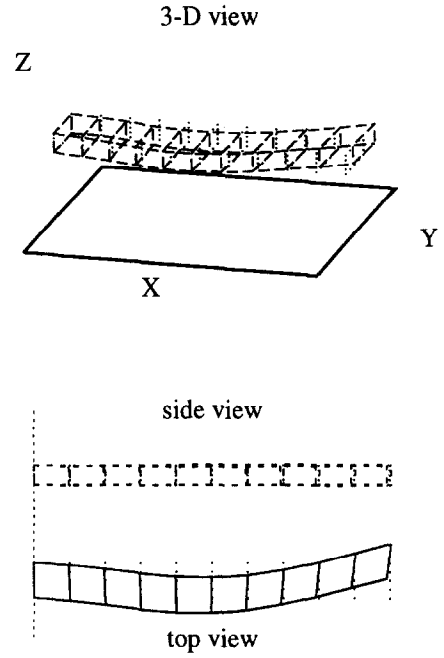

Fig. 11. Second chordwise bending mode of $[45°]_6$ thick-walled beam.

previous beam (see Table 1 and Table 2). As in the previous beam, for the first several modes there is no coupling between the beam bending, the chordwise bending and the torsional modes. However, for this thicker beam, a slight out-of-plane warping effect is noticed in the first chordwise bending mode (ω_{c1}), whose natural frequency is only 2.12 × larger the fundamental frequency ($\omega_o = 64.6$ Hz). The second chordwise bending mode ($\omega_{c2} = 11.5\ \omega_0$) is shown in Fig. 11. A significant amount of out-of-plane warping is observed in this mode predominantly due to the shearing in the upper and the lower walls. Figure 11 also shows that this mode is uncoupled, although its natural frequency is close to the first torsional mode ($\omega_{t1} = 11.0\ \omega_0$).

There is, however, a significant amount of coupling between the fourth beam bending mode ($\omega_{b4} = 28.40\ \omega_0$) and the third chordwise bending mode ($\omega_{c3} = 28.44\ \omega_0$). To illustrate this coupling, the third chordwise bending mode is shown in Fig. 12. This coupling, which is clearly due to the fact that their natural frequencies are very close, creates a significant amount of both inplane and out-of-plane warping as depicted in Fig. 12. Unlike the second chordwise bending mode which remains uncoupled from the nearby first torsion mode, the third chordwise bending mode seems to be coupled slightly with the second torsion mode ($\omega_{t2} = 30.2\ \omega_0$) as well as with the fourth beam bending mode.

Finally, to illustrate the importance of including both the inplane and out-of-plane warping in the beam formulation, the second extensional mode ($\omega_{e2} = 46.5\ \omega_o$) is presented in Fig. 13. A significant amount of warping in observed in this mode which is slightly coupled with the third torsion mode ($\omega_{t3} = 42.7\ \omega_0$) and is largely coupled with the fourth chordwise bending mode ($\omega_{t2} = 48.7\ \omega_0$). Unlike the previous modes which have primarily linear warping, both the inplane and out-of-plane warping in this mode are nonlinear. Of particular interest is the 'necking' effect observed near the cantilevered edge in the side view and the nonlinear out-of-plane cross-sectional camber

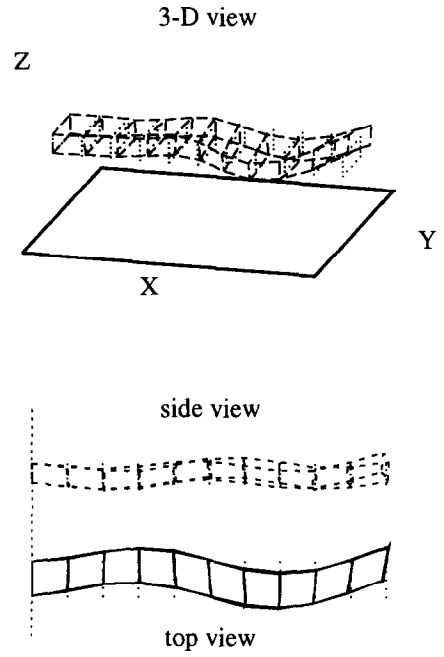

Fig. 12. Third chordwise bending mode of $[45°]_6$ thick-walled beam.

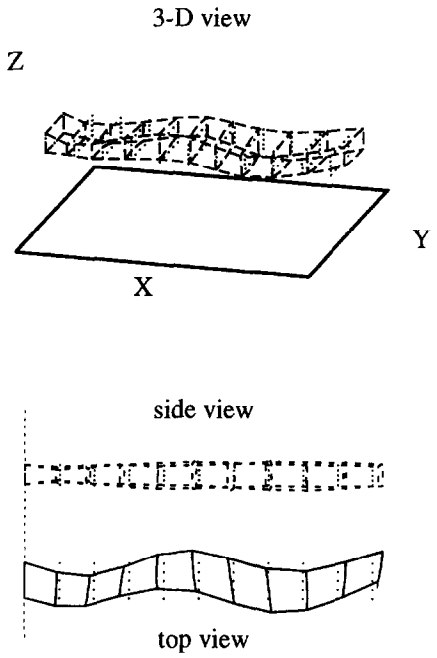

Fig. 13. Second extensional mode of $[45°]_6$ thick-walled beam.

which is demonstrated in the top view. This three-dimensional warping is a result of the shearing effects that are significant due to the thick-walled construction of the beam.

7. Concluding remarks

A new beam theory has been developed to model composite box beams with arbitrary wall thicknesses. The theory, which is based on higher-order composite laminate theory, approximates the three-dimensional elasticity solution rather than reducing the cross-sectional properties to one-dimensional beam properties. The developed theory automatically satisfies the stress-free boundary conditions on the inner and outer surfaces of the beam. Both inplane and out-of-plane warping are included in the formulation. The following important observations are made.

1. Very good agreement is observed between the static results and available experimental data for thin-walled beams.
2. The mode shapes are often highly coupled. The coupling is more noticeable in beams with thicker wall sections.
3. The beam theory captures the effects of inplane and out-of-plane warping. For thick-walled beams with low aspect ratios, the warping terms are significant even at the lower modes. For the thin-walled beams, the inplane warping is more important than the out-of-plane warping.
4. The increased warping in beams with thicker walls is due to transverse shear stresses through the thickness of the walls which increases with laminate thickness.

Acknowledgements

The authors would like to acknowledge support of this work through a grant from the NASA Ames Research Center, Grant Number NAG2-771, Technical Monitor Dr Sesi Kottapalli.

References

[1] Hodges DH, Ormiston RA, Peters DA. On the Nonlinear Deformation Geometry of Euler–Bernoulli Beams. NASA TP-1566, April 1980.
[2] Kosmatka JB, Friedmann PP. Vibration analysis of composite turbopropellers using a nonlinear beam-type finite-element approach. AIAA Journal 1989;27:(11):1606–1614.
[3] Stemple AD, Lee SW. Finite-element model for composite beams with arbitrary cross-sectional warping. AIAA Journal 1988;26:(12):1512–1520.
[4] Wörndle R. Calculation of the cross-section properties and the shear stresses of composite rotor blades. Vertica 1982;6:111–129.
[5] Cesnik CES, Sutyrin VG, Hodges DH. Refined theory of twisted and curved composite beams: the role of short-wavelength extrapolation. Paper No. AIAA 94-1451-CP, Proceedings, 35th Structures, Structural Dynamics, and Materials Conference, Hilton Head, South Carolina, April 18–20, 1994:1134–1143.
[6] Bauchau OA. A beam theory for anisotropic materials. Journal of Applied Mechanics 1985;52:416–422.
[7] Rand O. Theoretical modeling of composite rotating beams. Vertica 1990;14:(3):329–343.
[8] Rehfield LW, Atilgan AR, Hodges DH. Nonclassical behavior of thin-walled composite beams with closed cross-sections. Journal of the American Helicopter Society 1990;35:42–50.
[9] Smith EC, Chopra I. Formulation and evaluation of an analytical model for composite box-beams. Journal of the American Helicopter Society 1991;36:23–35.
[10] Kalfon JP and Rand O. Nonlinear analysis of composite thin-walled helicopter blades. Proceeding sof the 48th Annual Forum of the American Helicopter Society, Washington, D.C., 1992:1465–1478.
[11] Gu H, Chattopadhyay A. A new higher order plate theory in modeling delamination buckling of composite laminates. AIAA Journal 1994;32:1709–1716.
[12] Reddy JN. A general non-linear third-order theory of plates with moderate thickness. International Journal of Non-Linear Mechanics 1990;25:677–686.
[13] Reddy JN. Energy and Variational Principles in Applied Mechanics. New York: John Wiley and Sons, 1984.
[14] Chandra R, Stemple AD, Chopra I. Thin-walled composite beams under bending torsional and extensional loads. Journal of Aircraft 1990;27:619–626.
[15] Smith EC, Chopra I. Formulation and evaluation of an analytical model for composite box-beams. Journal of the American Helicopter Society 1991;36:(7):23–35.

Appendix A

Coordinate system relations

The transformation between the untwisted global coordinate system and the rotated coordinate system is expressed as follows.

$$\begin{Bmatrix} X' \\ Y' \\ Z' \end{Bmatrix} = \begin{bmatrix} 1 & 0 & 0 \\ 0 & \cos\theta & \sin\theta \\ 0 & -\sin\theta & \cos\theta \end{bmatrix} \begin{Bmatrix} X \\ Y \\ Z \end{Bmatrix} \tag{A1}$$

The two wall coordinate systems are written in terms of the two beam coordinate systems as

$$\begin{Bmatrix} x_i \\ y_i \\ z_i \end{Bmatrix} = \begin{Bmatrix} X_i \\ Y_i + Y_{o_i} \\ Z_i + Z_{o_i} \end{Bmatrix} \tag{A2}$$

and

$$\begin{Bmatrix} \chi_i \\ \eta_i \\ \zeta_i \end{Bmatrix} = \begin{Bmatrix} X'_i \\ Y'_i + Y'_{o_i} \\ Z'_i + Z'_{o_i} \end{Bmatrix} \tag{A3}$$

where the global coordinate system (X_i, Y_i, Z_i) is written with the subscript 'i' to indicate the fact that Y_i is always aligned with the reference (untwisted) width of the individual walls. Similarly, the rotated coordinate system (X'_i, Y'_i, Z'_i) is always aligned such that Y'_i is parallel to the rotated width of the individual wall. This notation is adopted so that the relationship between the global and local coordinate systems can be expressed using only a single set of equations. The quantities, Y_{0i}, Z_{0i}, Y'_{0i} and Z'_{0i} correspond to distance from the axis of rotation to the edge of the individual walls where the wall coordinate systems are defined. Using eqns (A1)–(A3), the local wall, twisted coordinate system is written as

$$\begin{Bmatrix} \chi_i \\ \eta_i \\ \zeta_i \end{Bmatrix} = \begin{bmatrix} 1 & 0 & 0 \\ 0 & \cos\theta & \sin\theta \\ 0 & -\sin\theta & \cos\theta \end{bmatrix} \begin{Bmatrix} x_i \\ y_i - Y_{o_i} \\ z_i - Z_{o_i} \end{Bmatrix} + \begin{Bmatrix} 0 \\ Y'_{o_i} \\ Z'_{o_i} \end{Bmatrix}. \tag{A4}$$

Note that in the above relationship, θ is a function of x and varies along the span. The Jacobian matrix between the local untwisted and local twisted coordinate systems is then expressed as

$$\mathbf{J} = \begin{bmatrix} \dfrac{\partial\chi}{\partial x} & \dfrac{\partial\eta}{\partial x} & \dfrac{\partial\zeta}{\partial x} \\ \dfrac{\partial\chi}{\partial y} & \dfrac{\partial\eta}{\partial y} & \dfrac{\partial\zeta}{\partial y} \\ \dfrac{\partial\chi}{\partial z} & \dfrac{\partial\eta}{\partial z} & \dfrac{\partial\zeta}{\partial z} \end{bmatrix} \tag{A5}$$

$$= \begin{bmatrix} 1 & (\zeta - Z'_o)\dfrac{\partial\theta}{\partial x} & -(\eta - Y'_o)\dfrac{\partial\theta}{\partial x} \\ 0 & \cos\theta & -\sin\theta \\ 0 & \sin\theta & \cos\theta \end{bmatrix}, \tag{A6}$$

where the subscript 'i' has been omitted for convenience. It is seen from eqn (A5), that the determinant of the Jacobian, **J**, is equal to one.

Appendix B

Strain definitions

The zeroth order inplane strains in the absence of pre-twist are defined as follows.

$$\begin{Bmatrix} e_1^0 \\ e_2^0 \\ e_6^0 \end{Bmatrix} = \begin{Bmatrix} u_{o,\chi} \\ v_{o,\eta} \\ u_{o,\eta} + v_{o,\chi} \end{Bmatrix} \tag{B1}$$

The first order inplane strains are

$$\begin{Bmatrix} \kappa_1^1 \\ \kappa_2^1 \\ \kappa_6^1 \end{Bmatrix} = \begin{Bmatrix} -w_{o,\chi\chi} + \psi_{x,\chi} \\ -w_{o,\eta\eta} + \psi_{y,\eta} \\ -2w_{o,\chi\eta} + \psi_{x,\eta} + \psi_{y,\chi} \end{Bmatrix}, \tag{B2}$$

and the third components of the inplane strain are

$$\begin{Bmatrix} \kappa_1^3 \\ \kappa_2^3 \\ \kappa_6^3 \end{Bmatrix} = -\frac{4}{3h^2} \begin{Bmatrix} \psi_{x,\chi} \\ \psi_{y,\eta} \\ \psi_{x,\eta} + \psi_{y,\chi} \end{Bmatrix}, \tag{B3}$$

The zeroth and the second order components of the out-of-plane strains are defined as follows.

$$\begin{Bmatrix} e_4^0 \\ e_5^0 \end{Bmatrix} = \begin{Bmatrix} \psi_y \\ \psi_x \end{Bmatrix} \tag{B4}$$

$$\begin{Bmatrix} \kappa_4^2 \\ \kappa_5^2 \end{Bmatrix} = -\frac{4}{h^2} \begin{Bmatrix} \psi_y \\ \psi_x \end{Bmatrix} \tag{B5}$$

The additional non-zero inplane strain components due to pre-twist are written as

$$\begin{Bmatrix} \mu_1^0 \\ \mu_6^0 \end{Bmatrix} = -\begin{Bmatrix} Z'_o u_{o,\eta} + (\eta - Y'_o)(-w_{o,\chi} + \psi_x) \\ Z'_o v_{o,\eta} + (\eta - Y'_o)(-w_{o,\eta} + \psi_y) + w_o \end{Bmatrix} \tag{B6}$$

$$\begin{Bmatrix} \mu_1^1 \\ \mu_6^1 \end{Bmatrix} = \begin{Bmatrix} u_{o,\eta} - Z'_o(-w_{o,\chi\eta} + \psi_{x,\eta}) \\ v_{o,\eta} - Z'_o(-w_{o,\eta\eta} + \psi_{y,\eta}) \end{Bmatrix} \tag{B7}$$

$$\begin{Bmatrix} \mu_1^2 \\ \mu_6^2 \end{Bmatrix} = \begin{Bmatrix} -w_{o,\chi\eta} + \psi_{x,\eta} + \dfrac{4}{h^2}(\eta - Y'_o)\psi_x \\ -w_{o,\eta\eta} + \psi_{y,\eta} + \dfrac{4}{h^2}(\eta - Y'_o)\psi_y \end{Bmatrix} \tag{B8}$$

$$\begin{Bmatrix} \mu_1^3 \\ \mu_6^3 \end{Bmatrix} = \begin{Bmatrix} \dfrac{4}{3h^2} Z'_o \psi_{x,\eta} \\ \dfrac{4}{3h^2} Z'_o \psi_{y,\eta} \end{Bmatrix} \tag{B9}$$

$$\begin{Bmatrix} \mu_1^4 \\ \mu_6^4 \end{Bmatrix} = \begin{Bmatrix} -\dfrac{4}{3h^2} \psi_{x,\eta} \\ -\dfrac{4}{3h^2} \psi_{y,\eta} \end{Bmatrix} \tag{B10}$$

Finally, the non-zero out-of-plane components of the strain due to presence of pre-twist are written as

$$\mu_5^0 = v_0 - Z_0' w_{0,\eta} \tag{B11}$$

$$\mu_5^1 = \psi_x \tag{B12}$$

$$\mu_5^3 = -\frac{4}{3h^2} \psi_x \tag{B13}$$